EPR, ENDOR, and TRIPLE resonance spectroscopy on the neutral flavin radical in Escherichia coli DNA photolyase

ARTICLE *in* BIOCHEMISTRY · DECEMBER 1999

Impact Factor: 3.02 · DOI: 10.1021/bi991442u · Source: PubMed

9 AUTHORS, INCLUDING:

Richard Feicht
Technische Universität München
14 PUBLICATIONS **398** CITATIONS
SEE PROFILE

Adelbert Bacher
Technische Universität München
597 PUBLICATIONS **16,336** CITATIONS
SEE PROFILE

Gerald Richter
Cardiff University
75 PUBLICATIONS **2,167** CITATIONS
SEE PROFILE

EPR, ENDOR, and TRIPLE Resonance Spectroscopy on the Neutral Flavin Radical in *Escherichia coli* DNA Photolyase†

Christopher W. M. Kay,‡ Richard Feicht,§ Kristina Schulz,‡ Peter Sadewater,‡ Aziz Sancar,|| Adelbert Bacher,§ Klaus Möbius,‡ Gerald Richter,*,§ and Stefan Weber*,‡

Free University Berlin, Institute of Experimental Physics, 14195 Berlin, Germany, Technical University Munich, Institute of Organic Chemistry and Biochemistry, 85747 Garching, Germany, and University of North Carolina, School of Medicine, Chapel Hill, North Carolina 27599, U.S.A.

ABSTRACT: Ultraviolet radiation promotes the formation of a cyclobutane ring between adjacent pyrimidine residues on the same DNA strand to form a pyrimidine dimer. Such dimers may be restored to their monomeric forms through the action of a light-absorbing enzyme named DNA photolyase. The redox-active cofactor involved in the light-induced electron transfer reactions of DNA repair and enzyme photoactivation is a noncovalently bound FAD. In this paper, the FAD cofactor of *Escherichia coli* DNA photolyase was characterized as the neutral flavin semiquinone by EPR spectroscopy at 9.68 and 94.5 GHz. From the high-frequency/high-field EPR spectrum, the principal values of the axially symmetric *g*-matrix of $FADH^{\bullet}$ were extracted. Both EPR spectra show an emerging hyperfine splitting of 0.85 mT that could be assigned to the isotropic hyperfine coupling constant (hfc) of the proton at N(5). To obtain more information about the electron spin density distribution ENDOR and TRIPLE resonance spectroscopies were applied. All major proton hfc's could be measured and unambiguously assigned to molecular positions at the isoalloxazin moiety of FAD. The isotropic hfc's of the protons at C(8α) and C(6) are among the smallest values reported for protein-bound neutral flavin semiquinones so far, suggesting a highly restricted delocalization of the unpaired electron spin on the isoalloxazin moiety. Two further hfc's have been detected and assigned to the inequivalent protons at C(1′). Some conclusions about the geometrical arrangement of the ribityl side chain with respect to the isoalloxazin ring could be drawn: Assuming tetrahedral angles at C(1′) the dihedral angle between the C(1′)−C(2′) bond and the $2p_z$ orbital at N(10) has been estimated to be 170.4° ± 1°.

Ultraviolet light (200−300 nm) typically damages nucleic acids by the formation of cis,syn-cyclobutane pyrimidine dimers (CPDs)[1] in cellular DNA that are potentially mutagenic, carcinogenic, and lethal in a variety of organisms. Cells are able to protect themselves against these types of damage by excision repair or by photoreactivation mediated by the enzyme DNA photolyase, also called CPD photolyase (*1*−*6*), present in many life forms. DNA photolyase has a high degree of amino acid sequence identity to the related (6−4) photolyase from *Drosophila*, which again is similar to homologues from plants and mammals named cryptochromes 1 and 2 (CRY1 and CRY2) (*7*). The latter, however, have no DNA repair activity, and it has been suggested that these pigments may function as photoreceptors for setting the circadian clock (*8*, *9*).

Recently, the crystal structures of DNA photolyase from two different organisms, *Escherichia coli* (*10*) and *Anacystis nidulans* (*11*), have been resolved at 2.3 Å and 1.8 Å resolution, respectively. While both enzymes utilize different chromophores as light harvesting cofactors (5,10-methenyltetrahydrofolylpolyglutamate in *E. coli* photolyase and 8-hydroxy-5-deazaflavin in *A. nidulans* photolyase), the redox-active site containing the catalytic cofactor flavin adenine dinucleotide (FAD, probably in its anionic form $FADH^-$) is highly conserved in both photolyases. At least two types of photoreactions have been observed experimentally in DNA photolyase: (1) photorepair of damaged DNA by the catalytically active enzyme with its flavin cofactor in the fully reduced state, $FADH^-$, and (2) photoactivation of the catalytically inert enzyme when its flavin cofactor is in a redox state different from $FADH^-$. For DNA repair, the enzyme selectively binds to the damaged segment of the DNA in a light-independent step. Restoration of DNA functionality by enzymatic splitting of the CPD into the individual pyrimidines has been recognized as light-induced electron transfer initiated by the absorption of near-UV or visible light (see Figure 1). In the photoactivation reaction, the flavin cofactor is reduced to its catalytic active form $FADH^-$ with the participation of the amino acid residue Trp-

† This work was supported by the Deutsche Forschungsgemeinschaft (DFG) (DFG Schwerpunkt-Programm "High-Field EPR" and SFB-533).

* Corresponding author. Stefan Weber, Free University Berlin, Institute of Experimental Physics, 14195 Berlin (Germany). Telephone: +49 (30) 838-6139. Fax: +49 (30) 838-6046. E-mail: stefan.weber@physik.fu-berlin.de. Gerald Richter, Technical University of Munich, Institute of Organic Chemistry and Biochemistry, 85747 Garching (Germany). Telephone: +49 (89) 289−13336. Fax: +49 (89) 289−13363. E-mail: gerald.richter@ch.tum.de.

‡ Free University Berlin, Germany.

§ Technical University Munich, Germany.

|| University of North Carolina.

[1] Abbreviations: EPR, electron paramagnetic resonance; ENDOR, electron−nuclear double resonance; TRIPLE, electron−nuclear−nuclear triple resonance; CPD, cyclobutane pyrimidine dimer; FAD, flavin adenine dinucleotide; $FADH^-$, fully reduced FAD anion; $FADH^{\bullet}$, neutral FAD radical; hf, hyperfine; hfc, hyperfine coupling constant; RF, radio frequency; cw, continuous-wave.

10.1021/bi991442u CCC: $18.00
Published on Web 11/25/1999

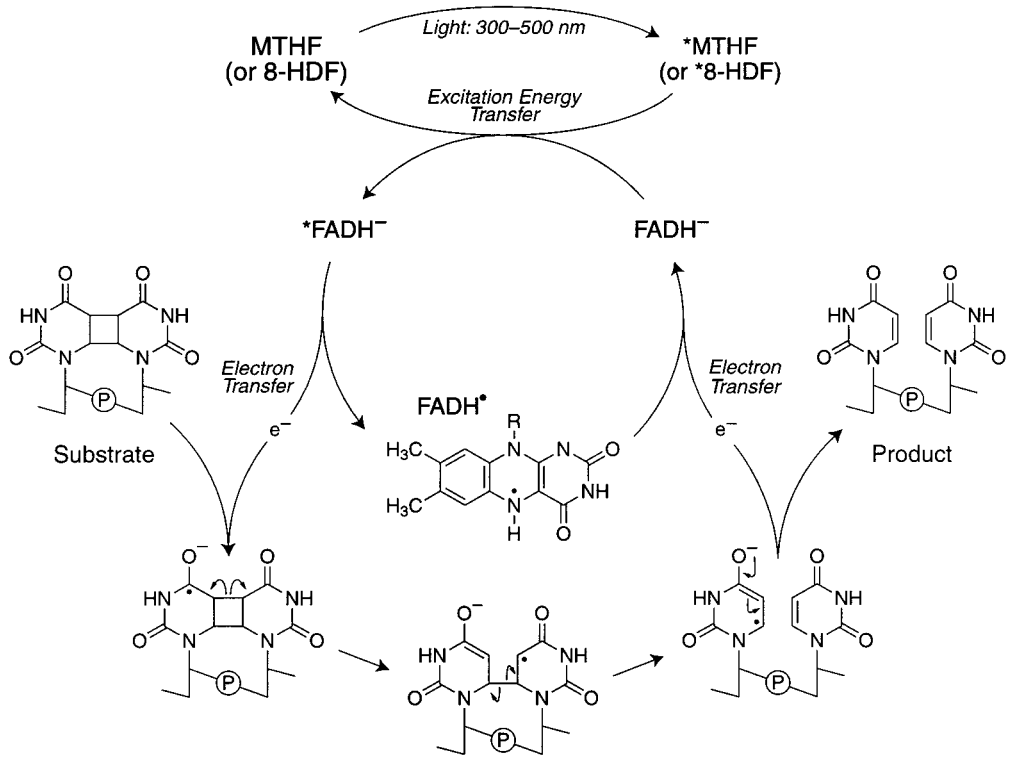

FIGURE 1: Putative reaction mechanism of DNA photolyase.

306, which is located approximately 14 Å away, close to the surface of the enzyme (*12*−*14*). In both electron-transfer processes, the flavin in its radical (semiquinone) form, FADH•, is involved either as an important intermediate in the overall catalytic pathway or as a possible electron acceptor for photoreduction. Therefore, a detailed knowledge of the magnetic interactions within this chromophore and with its protein environment which, in principle, can be extracted from electron paramagnetic resonance (EPR) data is especially useful for a mechanistic interpretation of both photoprocesses (*13*, *15*−*18*). In particular, the isotropic hyperfine coupling constant (hfc) of magnetic nuclei, A^i_{iso}, (where *i* is the type of nucleus, e.g. ^{1}H, ^{13}C, or ^{14}N) and the resulting line pattern of EPR and ENDOR (electron−nuclear double resonance) spectra contain valuable information on the molecular structure and the electron spin distribution in the paramagnetic species. The A^i_{iso} arise from the Fermi contact interaction between the unpaired electron and the nucleus (*19*). This is described in eq 1,

$$A^i_{iso} = \frac{2}{3} g_e g_n \mu_B \mu_n \mu_0 (1/(h a_0^3)) Q^i(0), \qquad (1)$$

where A^i_{iso} is measured in Hz, g_e and g_n are the electron and nuclear *g*-factors, μ_B and μ_n are the Bohr and the nuclear magneton, respectively, μ_0 is the vacuum permeability, *h* is the Planck constant, a_0 is the Bohr radius, and $Q^i(0)$ is the spin density at nucleus *i*.

In this investigation, we take advantage of the fact that the flavin cofactor in DNA photolyase is oxidized into its semiquinone form during enzyme isolation and purification in an aerobic environment. A stable EPR signal in DNA photolyase was first reported by Jorns et al. (20) and, based on its peak-to-peak line width of 1.9 mT, attributed to a neutral flavin radical, FADH•. Subsequently, the same signal centered at around $g = 2.0038$ has been published by several groups (*13*, *15*−*18*), however, no interpretation of the line width and the emerging hyperfine (hf) structure has been given so far. To increase spectral resolution, we have reexamined the EPR signal of the FAD cofactor in DNA photolyase using ENDOR (*21*) and electron−nuclear−nuclear triple (TRIPLE) resonance (*22*). In ENDOR, an EPR transition is saturated, which leads to a collapse of the observed EPR signal as the corresponding state populations equalize. If one now simultaneously irradiates the spin system with a radio frequency (RF) field in order to induce transitions between the nuclear sublevels, i.e., NMR (nuclear magnetic resonance) transitions, the condition of saturation in the EPR transition is lifted as the nuclear sublevel populations shift, and there is a partial recovery of the EPR signal. Typically, hfc's may be obtained from ENDOR even when the EPR signal is inhomogeneously broadened and no hf structure is resolved. A refinement of the ENDOR experiment is electron−nuclear−nuclear triple resonance, now commonly denoted as TRIPLE. In General TRIPLE experiments, one monitors the effect of a simultaneous excitation of two nuclear spin transitions on the level of the EPR absorption. From the characteristic intensity changes of the high-frequency and low-frequency signals compared with those of the ENDOR signals, the relative signs of the hfc's can easily be determined (*22*).

In the present paper, we focus on hf interactions arising from protons attached to the isoalloxazin moiety of the FAD cofactor in DNA photolyase. From our EPR and ENDOR/TRIPLE experiments, we can get new, valuable data about spin density distributions in the benzene and pyrazine rings of the flavin. The characterization of flavin semiquinones by these techniques offers more possibilities in the study of the structural arrangement of the cofactor in its protein environment.

Table 1: Bacterial Strains and Plasmids

strain/plasmid	relevant characteristics	source
Escherichia coli strains:		
M15(pRep4)	lac,ara,gal,mtl,recA$^+$,uvr$^+$ [pRep4,lacI,kan^r]	(*23*)
RR28	F$^-$,thi,pro,lac,gal,ara,mtl,xyl,supE44,endA,hsd(r$^-$,m$^-$),pheS,recA	(*24*)
plasmids:		
pNCO113	expression vector	(*25*, *26*)
pEPHR	pNCO113 with the *phr* gene of *E. coli*	this study

Table 2: Oligonucleotides Used for Construction of the Expression Plasmid pEPHR

oligonucleotide	cutting site	primer sequence
PLY1		GGAGAAATTAACTATGACTACCCATC
PLY2	*Bam*HI	TCACGCCGGATCCGGCATCTGG
P2	*Eco*RI	ACACAGAATTCATTAAAGAGGAGAAATTAACTATG

MATERIALS AND METHODS

Biological Material. Restriction enzymes and DNA ligase were purchased from New England BioLabs (Schwalbach, Germany) and from Roche Diagnostics (Mannheim, Germany). Taq polymerase was obtained from Eurogentec (Seraing, Belgium). Dithiothreitol (DTT) was purchased from Sigma (Deisenhofen, Germany). Oligonucleotides were custom-synthesized by MWG Biotech (Ebersberg, Germany). Microorganisms and plasmid vectors are summarized in Table 1. *Buffers.* Buffer A contained 50 mM 2-[4-(2-hydroxyethyl)-1-piperazino]-ethanesulfonic acid (HEPES), pH 7.0, 10 mM DTT, 100 mM NaCl and 10% (w/v) sucrose. Buffer B contained 50 mM HEPES, pH 7.0, 10 mM DTT and 10% (v/v) glycerol. Supplements were added as indicated.

Construction of the DNA Photolyase Hyperexpression Strain. The open reading frame of the *phr* gene was amplified by a strategy using two polymerase chain reaction (PCR) steps (*26*). Primers PLY1 and PLY2 (see Table 2) were designed according to the published sequence (*27*) (Genbank/EMBL accession number K01298) and used in the first PCR and chromosomal *E. coli* DNA strain RR28 as template. Primers P2 and PLY2 (see Table 2) and the product of the first PCR were used in the second. The resulting fragment was digested with restriction endonucleases *Eco*RI and *Bam*HI and ligated into the expression vector pNCO113 treated with the same enzymes. The ligation mixture was electrotransformed into *E. coli* M15(pRep4) cells, which were then plated on LB agar containing 150 mg of ampicillin and 15 mg of kanamycin/L. The resulting plasmid is subsequently designated pEPHR.

Cultivation of Bacterial Cells. The recombinant *E. coli* strain harboring plasmid pEPHR was cultured in baffled 2 L Erlenmeyer flasks containing 500 mL of LB medium supplemented with 150 mg of ampicillin and 15 mg of kanamycin/L. The cultures were incubated at 37 °C with shaking. At an optical density of 0.8 at 600 nm, isopropyl-thio-β-D-galactopyranoside (IPTG) was added to a final concentration of 1 mM, and incubation was continued for 5 h. The cells were harvested by centrifugation and stored at −20 °C.

Isolation of DNA Photolyase. Bacterial cell mass (17.5 g) was thawed in 25 mL of buffer A. The suspension was ultrasonically treated and centrifuged at 4 °C. The supernatant was placed on a column of Blue Sepharose CL-6B (Pharmacia, Freiburg, Germany) (2.5 × 9 cm), which was developed with a gradient of 0.1−2 M potassium chloride in buffer B. Blue-colored fractions were combined, and ammonium sulfate was added (0.43 g/mL). The precipitate was harvested by centrifugation and dissolved in buffer B containing 50 mM NaCl. The solution was placed on a desalting column HiPrep 26/10 (Pharmacia, Freiburg, Germany). Blue-colored fractions were combined and placed on a column of Heparin Sepharose CL-6B (2.5 × 8 cm) (Pharmacia, Freiburg, Germany), which was developed with a gradient of 0.1−1 M of KCl in buffer B. Fractions were combined and concentrated by ultrafiltration using C30 membranes from Amicon (Witter, Germany). Blue fractions were collected and glycerol was added to a final concentration of 50% (v/v). The solution was stored at −70 °C.

Buffer Exchange. Samples were transferred into the desired buffer (usually 50 mM HEPES in H_2O/glycerol (pH 7.0) or HEPES in D_2O/glycerol-D_3 (pD 7.0)) by dilution and ultrafiltration through C30 microconcentrators at 4 °C. The cycle was repeated five times to give a final buffer or D_2O enrichment of 95−99%.

EPR Sample Preparation. The enzyme preparations were transferred into EPR quartz tubes (3 mm i.d. for X-band EPR; 0.6 mm i.d. for W-band EPR) under an argon inert gas atmosphere in the dark. The enzyme was frozen rapidly with liquid nitrogen and stored therein. No changes in EPR/ENDOR signal line shapes and intensities have been observed over a time period of several months.

EPR Instrumentation. Continuous-wave (cw) EPR spectra at X-band frequencies (9−10 GHz) were obtained using a laboratory-built spectrometer. It consists of a Bruker ER041 MR microwave bridge and a Varian E-9 magnet. Samples were placed in a Bruker ER 4118X-MD-5W1 dielectric resonator, which was immersed in a laboratory-built helium gas flow cryostat.

W-band cw EPR spectra were recorded with a laboratory-built high-field/high-frequency EPR spectrometer operating at 94−96 GHz and equipped with a cylindrical TE_{011} cavity (*28*, *29*). The six-line EPR signal of a Mn(II)/MgO standard, placed near the sample in the cavity, was recorded simultaneously for *g*-factor calibration.

ENDOR Instrumentation. ENDOR and TRIPLE resonance spectra were recorded using an X-band spectrometer consisting of an AEG-20 electromagnet and a Bruker ER041 MR microwave bridge, in conjunction with a laboratory-built TM_{110} ENDOR cavity ($Q \simeq 1400$, 1 turn per mm NMR coil). An RF synthesizer (Hewlett-Packard 8660c) in conjunction

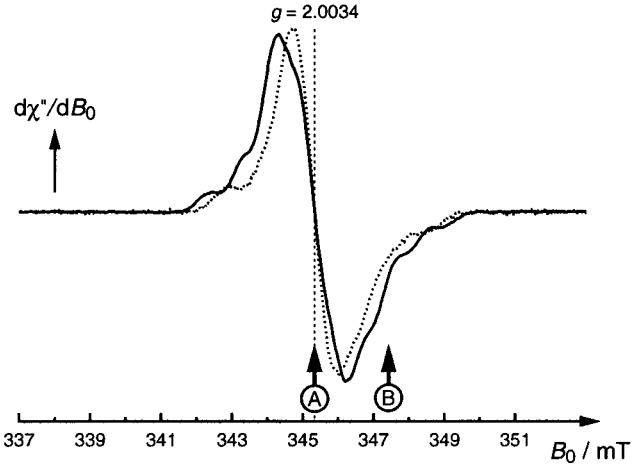

FIGURE 2: X-band cw-EPR frozen-solution spectra of *E. coli* DNA photolyase in protonated (solid line) and deuterated buffer (dotted line) with the flavin cofactor in the neutral semiquinone form. Spectra were recorded at 200 K with microwave power 6.1 μW, microwave frequency 9.6832 GHz, modulation amplitude 0.1 mT (100 kHz field modulation). The arrows indicate field positions at which ENDOR and TRIPLE spectra were recorded (see Figures 4−6), A center, B off-center field positions.

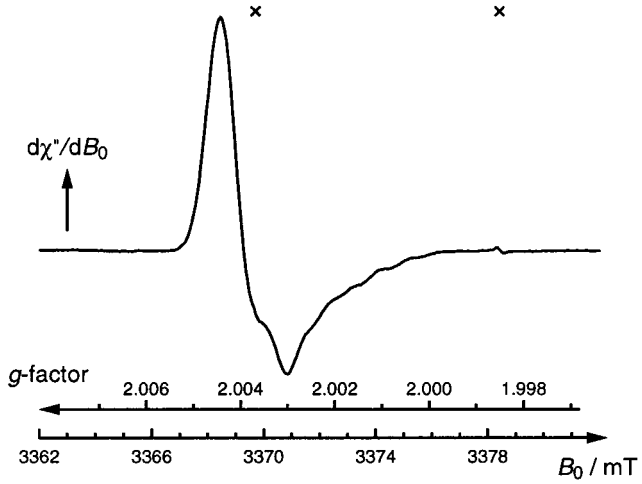

FIGURE 3: W-band cw-EPR frozen-solution spectrum of *E. coli* DNA photolyase in protonated buffer with the flavin cofactor in the neutral semiquinone form. The spectrum was recorded at 135 K with microwave power 50 μW, microwave frequency 94.50 GHz, modulation amplitude 0.1 mT (8 kHz field modulation). The EPR lines belonging to the Mn(II)/MgO standard used for *g*-factor calibration are indicated with crosses.

with a high-power RF amplifier (ENI A-300) was used to generate the cw B_2 field in the TM_{110} ENDOR cavity. Spectra were recorded at different temperatures between 120−230 K using a nitrogen gas flow adjusted by a Bruker ER4111 VT temperature controller.

RESULTS AND DISCUSSION

The *phr* gene of *E. coli* was cloned into the expression vector pNCO113 under the control of a *lac* operator and phage T_5 promoter yielding the plasmid pEPHR. Expression in this vector/host system was established to augment the yield of DNA photolyase, thus enabling future experiments with stable isotope incorporation into apoprotein and cofactor. Recombinant *E. coli* strains carrying plasmid pEPHR expressed DNA photolyase to a level of about 10% of total soluble protein after induction with IPTG. The recombinant DNA photolyase (blue radical form) was isolated by a sequence of three chromatographic steps. The entire purification procedure is routinely carried out in a single day. The enzyme can be stored without loss of activity at −70 °C.

The UV−vis spectrum of $FADH^{\bullet}$ in DNA photolyase exhibits characteristic absorption bands at 500, 580, and 625 nm, rendering the enzyme blue at higher concentrations (*13*, *20*). Since the flavin cofactor in its fully reduced form and in its fully oxidized form does not exhibit any appreciable absorption above 450 and 500 nm, respectively, the composition of the enzyme preparation can be easily characterized by its UV−vis spectrum.

EPR Spectroscopy. The stable X-band EPR signal of the flavin cofactor in *E. coli* DNA photolyase in its neutral radical form, $FADH^{\bullet}$, is shown in Figure 2. The peak-to-peak line width of 1.87 mT is in very good agreement with values observed by other groups (*13*, *15*−*18*, *20*). The line width of the signal is attributed to the mostly unresolved contributions of hfc's to ^1H and ^{14}N nuclei of the isoalloxazin moiety of the flavin cofactor as well as of the protein environment. In the case of neutral flavin semiquinones, the strong hfc of the proton at nitrogen N(5) contributes to the overall peak-to-peak line width of typically 2.0 mT, whereas in anionic flavin semiquinones, which are unprotonated at N(5), values of about 1.5 mT are usually observed.

The cw EPR signal is centered at $g = 2.0034$. This is close to the isotropic *g*-value of $FADH^{\bullet}$ obtained by analysis of the W-band EPR signal shown in Figure 3. At 94.50 GHz, a line shape characteristic for a randomly oriented radical with a *g*-matrix of axial symmetry is observed. From a preliminary spectrum simulation (data not shown), the principal values $g_\perp = 2.0043$ and $g_\parallel = 2.0022$ of the *g*-matrix have been extracted, corresponding to an average *g*-factor of $g_{iso} = 2.0036$.

In both W-band and X-band EPR spectra some hf structure emerges. Although not very clearly resolved, a spacing of 0.85 mT between adjacent shoulders in the signals could be determined. We have assigned this splitting to the isotropic hfc of the proton at the N(5) position. In the W-band EPR spectrum, the 0.85 mT-splitting is shifted to higher magnetic fields (see Figure 3). In this spectral region mostly molecules with the *Z* principal axis of the *g*-matrix (corresponding to the principal value $g_{ZZ} = g_\parallel = 2.0022$) aligned parallel to the direction of the external magnetic field are on resonance. In quinones and related molecules, the *Z*-axis is oriented perpendicular to the molecular plane of the π-ring system. Hence, that particular component of the hf tensor is selected that has its principal axis aligned parallel to *Z*. For α-protons attached to a π-ring system, this is the direction where the dipolar hf contribution is smallest. Therefore, at g_{ZZ}, a splitting close to A_{iso} is expected.

Additional evidence comes from the measurement of the cw EPR spectrum of the DNA photolyase enzyme in deuterated buffer where the strong hfc to the proton at N(5) can be eliminated by the exchange of the proton with deuterium (Figure 2). In D_2O, the EPR line width decreased to only 1.30 mT, giving further support for the notion of the existence of a neutral flavin radical in DNA photolyase. Moreover, the partly resolved splitting disappeared, revealing two clearly resolved outer hf lines that probably arise from the strongly coupled nitrogens at the 5 and 10 positions. The

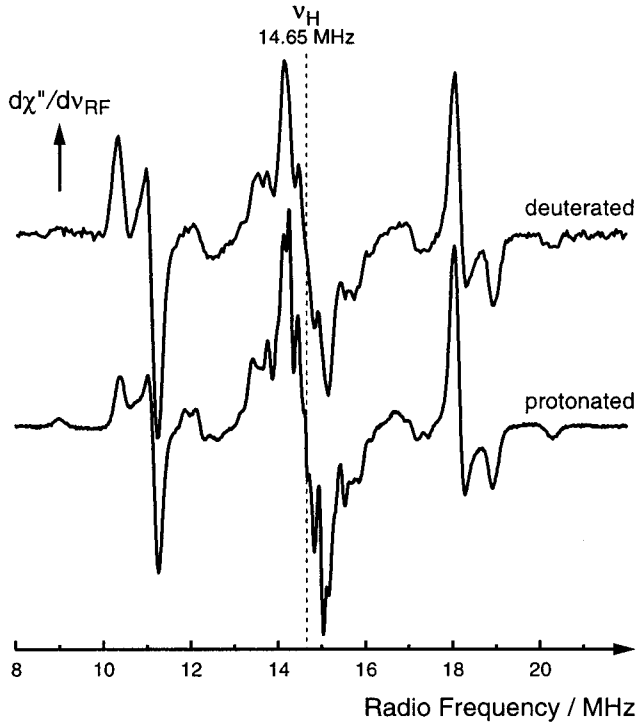

FIGURE 4: X-Band cw-ENDOR frozen-solution spectra of *E. coli* DNA photolyase in protonated (lower) and deuterated (upper) buffer. Spectra were recorded at 160 K with microwave power 2.5 mW, microwave frequency 9.6485 GHz, magnetic field 344.095 mT ($g = 2.0034$), radio frequency modulation amplitude 40 kHz (19 kHz frequency modulation).

cw EPR signal of DNA photolyase in deuterated buffer becomes more asymmetric due to the reduced inhomogeneous line width disclosing *g* anisotropies.

ENDOR/TRIPLE Spectroscopy. The ENDOR spectrum of the flavin cofactor in DNA photolyase in its neutral radical form, FADH•, recorded at a magnetic field corresponding to $g = 2.0034$ is shown in Figure 4. The frozen samples give rise to powder-type spectra that are symmetrical, centered around the proton Larmor frequency, ν_H.

"Matrix" Region. A group of signals with hf couplings ($|A| < 2.5$ MHz) in the so-called "matrix" region is the sum of contributions from weakly coupled protons of solvent water, protons from amino acid residues on the protein near the cofactor binding site and protons on the C(7α), C(9), and N(3) positions of the isoalloxazine ring. Studies on model compounds as well as molecular orbital calculations have demonstrated that for neutral flavin semiquinones hfc's from protons attached to C(7α), C(9), and N(3) are not expected to be larger than 1−2 MHz, since the spin densities estimated on such nuclei in the isoalloxazin ring are close to zero (*30*−*32*). Purely dipolar hf interactions arising from protons of hydrogen-bound amino acids and solvent water molecules close to the flavin ring may be identified by H/D exchange. ENDOR spectra of DNA photolyase in protonated and deuterated buffer (Figure 4) actually exhibit significant differences in the matrix region. An unambiguous assignment of these hfc's, however, will require a more systematic examination of the enzyme using isotope-labeling as well as point-mutations of the amino acid sequence and is, therefore, not in the scope of this contribution. Here, we will focus on the interpretation of hfc's that can be clearly assigned to specific nuclei within the flavin cofactor.

Table 3: Hyperfine Couplings[a] to Flavin Protons in *Escherichia coli* DNA Photolyase

atom position	$A_\perp$/MHz	$A_\parallel$/MHz	A_{iso}/MHz
N(5)*H*			−23[b]
C(6)*H*			−4.86[c]
C(8α)H_3	6.97	8.52	7.49
H^wC(1′)H^s	7.9	11.3	9.0
H^wC(1′)H^s	2.5	3.0	2.7

[a] All hfc's measured by ENDOR are accurate within ±0.1 MHz. [b] From EPR spectra (error ±1 MHz). [c] Negative sign determined by General TRIPLE resonance. For the labeling of the atom positions, see Figure 7.

C(8α) Methyl Protons and C(6) Proton hfc's. A second group of ENDOR signals due to more strongly coupled protons is observed in the regions 8.5−13.5 MHz and 15.5−20.5 MHz. The most pronounced signals therein are those indicating axial symmetry typical for the methyl group at C(8) (see Table 3). The large hfc with its two well-resolved $A_\perp$ and $A_\parallel$ components exhibits only a small hf anisotropy due to the free rotation of the methyl group. The isotropic hfc, A_{iso}, which is directly related to the spin density on these nuclei (see eq 1) can be determined from $A_{iso} = (2A_\perp + A_\parallel)/3$, and has a value of 7.49 MHz. Interestingly, the intensities of the features belonging to the $A_\parallel$ component of the C(8α) methyl group at $\nu_H \pm A_\parallel/2$ increase with respect to the corresponding $A_\perp$ component when the enzyme is transferred into deuterated buffer. No other changes are observed in the regions 8.5−13.5 MHz and 15.5−20.5 MHz upon H/D-exchange. Therefore, we conclude that a negative going feature at $\nu_H - A_\parallel/2$ and a positive going feature at $\nu_H + A_\parallel/2$ is superimposed on the C(8α) methyl group signal in the ENDOR spectra of the enzyme in protonated buffer. The lines are assigned to one component of the hf tensor of the strongly coupled proton at N(5) for which an isotropic hfc of 0.85 mT (23 MHz) has been determined from the EPR spectra (see above). Normally, it is very difficult to detect these resonances because of the large hf anisotropy for α-protons: The resonance region is smeared out over a large frequency range, typically from $0.5A_{iso}$ to $1.5A_{iso}$ with pronounced spectral features expected at $0.5A_{iso}$, A_{iso}, and $1.5A_{iso}$ (*33*). Having found features at 23 MHz (from EPR spectroscopy) and 8.5 MHz (from the ENDOR spectra) implies an even bigger hf anisotropy for the proton at N(5). This, however, seems not to be unreasonable given the highly unequal electronic spin density distribution on the three rings of the isoalloxazin system (see below) that is probed by the proton at the N(5) position.

Another hfc could be detected and assigned to the proton at C(6). This signal is expected to be of rhombic shape and, because of its high hf anisotropy, to be relatively weak. Usually only single features of such a hf tensor are observable. From Figure 4, we cannot resolve other features than the central crossing point of the rhombic pattern at 12.22 and 17.08 MHz, and so the magnitude of A_{iso} is only approximate. Additional evidence for this assignment comes from General TRIPLE resonance spectra of FADH• in DNA photolyase (see Figure 5A): When applying a second continuous RF field at 18.7 MHz where the C(8α) methyl protons are on resonance, the A_{iso} signal of the proton at C(6) is enhanced. A signal enhancement on the same side of the frequency axis (with respect to the free proton line) as the

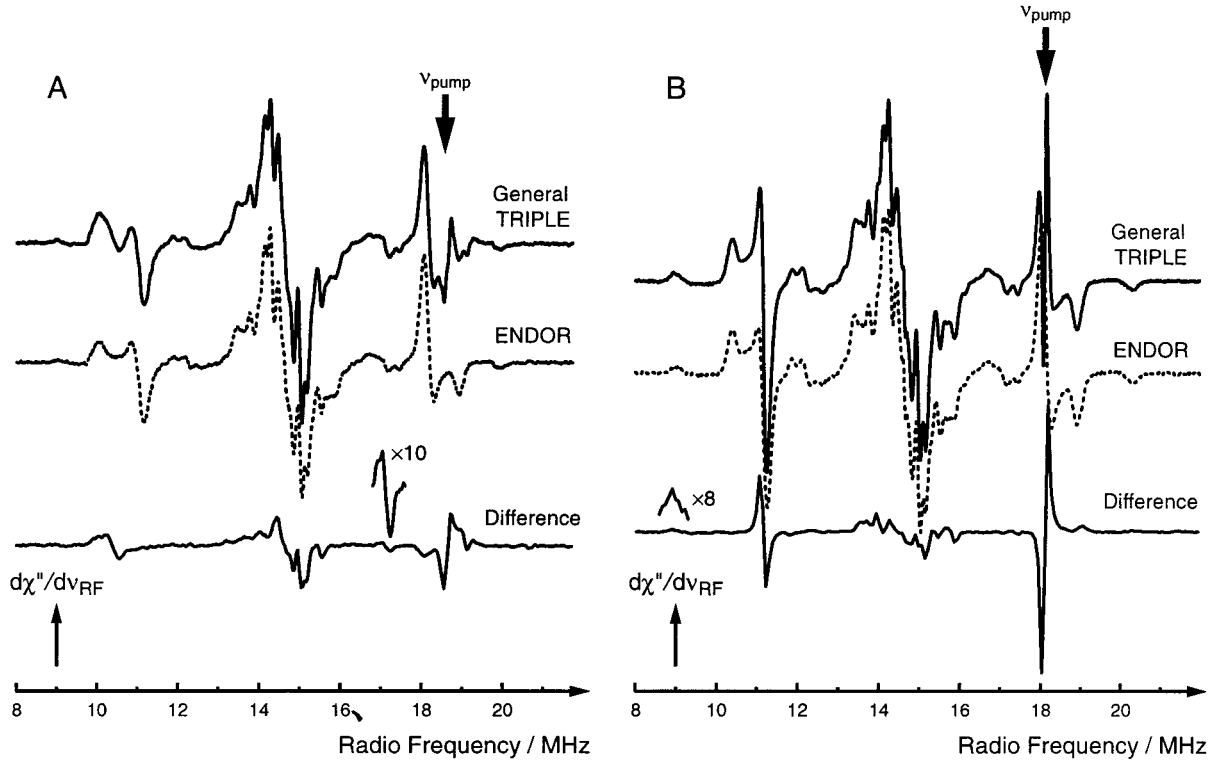

FIGURE 5: X-Band cw General TRIPLE spectra of *E. coli* DNA photolyase in protonated buffer, recorded using different pump frequencies ν_{pump} (A) 18.7 MHz, and (B) 18.0 MHz. From the characteristic intensity changes of the high-frequency and low-frequency signals compared with those of the ENDOR signals the relative signs of the hfc's can be determined.

pump frequency indicates an opposite sign for the hfc of the enhanced signal compared to the hfc being pumped (*22*). From molecular orbital calculations, it is known that the C(8α) methyl proton hfc has a positive sign, therefore, a negative sign for the proton hfc at C(6) is obtained from our experiments, in accordance with expectations on theoretical grounds (*32*).

It has been shown that both the C(8α) methyl proton and the C(6) proton hfc's are sensitive indicators for the spin density distribution in flavins. Hence, they can be used to probe the shifts of electron spin density over the isoalloxazin moiety which may occur after substrate binding to flavoenzymes (*32*, *34*−*38*). The isotropic hfc's of the C(8α) methyl protons and the C(6) proton of the flavin cofactor in DNA photolyase (see Table 3) are among the smallest values reported for neutral flavin semiquinones in flavoproteins so far. Therefore, our ENDOR studies reveal that in FADH• of DNA photolyase the unpaired spin density is significantly shifted to the central pyrazine ring and the outer pyrimidine ring of the isoalloxazine moiety. One possible reason for this peculiarity might be the specific location of the FAD cofactor in the protein: The pyrimidine part of the isoalloxazine ring is directed toward the interior of the enzyme; in particular, it is covered by the polar amino acids Asp-372 and Arg-344 that are mutually hydrogen bonded (*10*). The benzene fragment at the opposite part of the isoalloxazin moiety, however, points toward the putative substrate binding pocket and, driven by its hydrophobicity, facilitates the docking of the enzyme to the CPD in the DNA substrate. The absence of any stabilizing amino acid residues, such as tyrosines or tryptophanes, near this part of the flavin, therefore, does not promote distribution of the unpaired spin over the entire isoalloxazine moiety. This might have some interesting functional implications: Once an electron is transferred from the reduced flavin, $FADH^-$, to the CPD and a transient FADH• radical is formed, the rather poor stabilization of the unpaired electron spin over the isoalloxazine moiety might favor back-transfer of the electron from the then split pyrimidine dimers to the flavin. To what extent the unique U-shaped conformation of the FADH• in DNA photolyase (*10*, *11*) plays an important part in the spin density distribution remains to be clarified. The FAD molecule in the enzyme is bent in such a way that the isoalloxazine and adenosine moieties are facing each other. The conformation of the photolyase cofactor seems to be unique as it differs fundamentally from "classical" binding conformations, which show FAD in an elongated structure. This difference in binding conformation may be reflected by the differences of the spin densities observed here when compared with FAD cofactors in other flavoproteins.

C(1′) Proton hfc's. Two different hfc's are expected for the two β-protons at position C(1′). This effect is caused by the hindered rotation of the hydroxyalkyl side chain about the C(1′)−N(10) axis rendering both protons magnetically inequivalent. The distance of these protons to the nitrogen at position 10 (which carries a high spin density) is rather large and the anisotropic dipolar coupling is, therefore, relatively small. They may have a large contact hf interaction A_{iso}, however, which varies with the twist angle θ between the N(10) $2p_z$-orbital and the plane defined by the N(10)−C(1′) bond and the respective C(1′)−H bond (see below). A $\cos^2\theta$ dependence of the splitting is expected if the coupling is caused by hyperconjugation (*39*, *40*). ENDOR studies on other protein-bound neutral flavin semiquinones have shown that one of the two β-protons is more strongly coupled than the other and exhibits isotropic hfc's in a range of 10−14.5

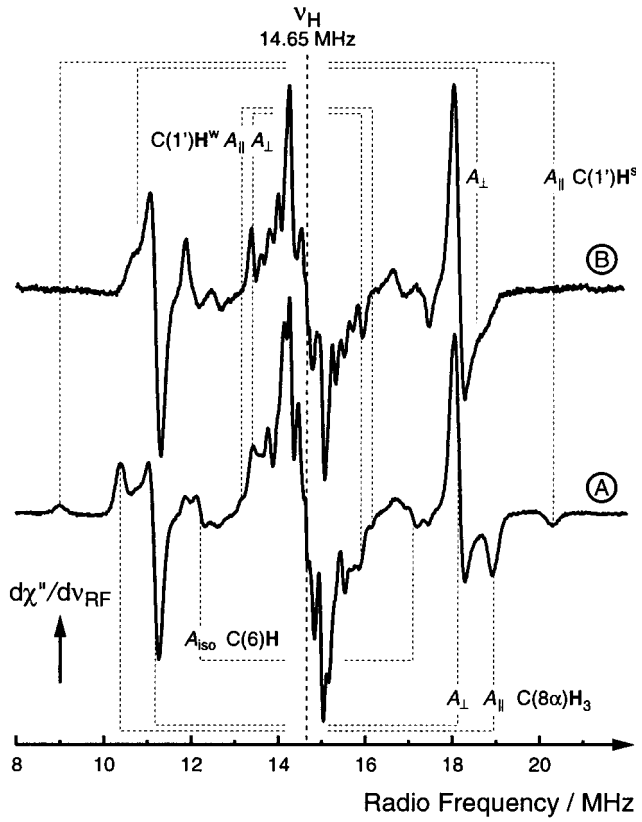

FIGURE 6: X-Band cw-ENDOR spectra of *E. coli* DNA photolyase in protonated buffer recorded at 344.095 mT (lower, $g = 2.0034$, see arrow A in Figure 2) and 346.195 mT (upper, off-center magnetic field setting, see arrow B in Figure 2). Other parameters as in Figure 4.

MHz. For the second more weakly coupled proton, hfc's in a narrow frequency range of 2.5−4 MHz are expected (*32*, *34*). In the following, we will refer to the β-protons at C(1′) as H^s and H^w where the superscript indicates strong and weak hfc, respectively.

Two groups of signals with an axial symmetry and a small hf anisotropy are observed in the ENDOR spectra shown in Figure 4. An unambiguous identification of the lines belonging to the two (inequivalent) protons at C(1′) is accomplished utilizing orientation selection effects that appear when ENDOR spectra are recorded at off-center magnetic field positions of the EPR spectrum (see Figure 6) as indicated in Figure 2. The outer parts of the FADH$^\bullet$ EPR signal predominantly arise from molecules with ^{14}N M_I values of either +1 or −1 that have their molecular plane perpendicular to the magnetic field. Hence, by desaturation of the spectral wings of the EPR signal, single-crystal like ENDOR spectra can be expected where only those components of the proton hf tensors can be detected that have their axes parallel to the respective component of the dominating ^{14}N hf tensor (N(5) or N(10)) (see Figure 6). In the case of the methyl group at C(8), this is the $A_\perp$ component (perpendicular to the cylindrical axis of the rotating methyl group). Similar selection principles apply for the β-protons at C(1′). From the two ENDOR lines with hf couplings of 11.3 MHz and 7.9 MHz, only the latter can be detected at off-center field settings. Therefore, these two signals may be assigned as the $A_\parallel$ and $A_\perp$ components of the hf tensor of H^s, respectively (see Table 3). An isotropic hfc of 9.0 MHz is calculated from these values. A positive sign of this hfc has been determined by General TRIPLE resonance (see Figure 5B) in accordance with theoretical expectations: A signal enhancement at 9.0 MHz (opposite to the side of the frequency axis where the second pump RF is applied) is observed, which indicates that the hf coupling of the signal being enhanced is equal to the sign of the hf coupling of the signal being pumped (here, the C(8α) methyl protons).

Performing ENDOR experiments at off-center field settings has proven to be useful in this particular case as the $A_\perp$ component of H^s overlaps with the signal of the C(8α) methyl group in the ENDOR spectrum taken in the center part of the EPR signal. A deconvolution of the two signals becomes feasible by exploiting the orientational selection.

We have applied the same procedure to identify the hfc of the weakly coupled proton H^w at C(1′) even though the assignment is more difficult due to the small size of the coupling. Nevertheless, a value of 2.7 MHz for A_{iso} (see Table 3) could be obtained for this nucleus in accordance with the following evidence. First, both the $A_\parallel$ and $A_\perp$ features can still be observed after H/D buffer exchange (see Figure 4) demonstrating that the corresponding proton is neither exchangeable nor a "true" matrix proton. Second, a positive sign of this hfc has been determined from General TRIPLE (see Figure 5), indicating that the coupling is derived from a β-proton. Third, the possibility that these features arise from the methyl group at C(7) can be discounted; molecular orbital calculations have shown that the hfc from this group is close to zero. Finally, in the orientation selection experiment (see Figure 6) only the outer $A_\parallel$-feature disappears in accordance with expectation (see above).

For the β-protons at C(1′) in FADH$^\bullet$, the isotropic hfc as a function of the radical geometry may be expressed as (*39*, *40*)

$$A_{iso}^i = C_0 + C_2 \cos^2 \theta^i, \qquad (2)$$

where θ^i is the dihedral angle between the C(1′)−H^i bond ($i = s, w$) and the N(10) $2p_z$ orbital, both projected on a plane perpendicular to the N(10)−C(1′) bond. Theoretical calculations of methyl proton hf interactions have shown that $C_0 \ll C_2$, and therefore, negligible as long as θ^i is not too close to 90°. Under these assumptions,

$$\frac{A_{iso}^s}{A_{iso}^w} = \frac{\cos^2 \theta^s}{\cos^2 \theta^w} \qquad (3)$$

can be derived from eq 2. We assume that all the bond angles at C(1′) are tetrahedral, therefore, $\theta^s + \theta^w = 120°$ (see Figure 7). With the isotropic hfc's for H^s and H^w (see Table 3) the dihedral angles $\theta^s = 50.4 \pm 0.5°$ and $\theta^w = 69.6 \pm 0.5°$ are obtained for the C−H^s bond and C−H^w bond, respectively. There are four equivalent arrangements of H^s and H^w with respect to the plane defined by the N(10) $2p_z$ orbital and the N(10)−C(1′) bond that cannot be distinguished from our experiments. By comparison with the X-ray structures of DNA photolyase from *E. coli* (*10*) and *A. nidulans* (*11*), however, one solution is strongly favored in which the hydroxyalkyl side chain points to the back right-hand side when viewing the isoalloxazin moiety as is indicated in Figure 7. From this result, we can determine a dihedral angle of $\phi = 170.4 \pm 1°$ between the C(1′)−C(2′) bond and the

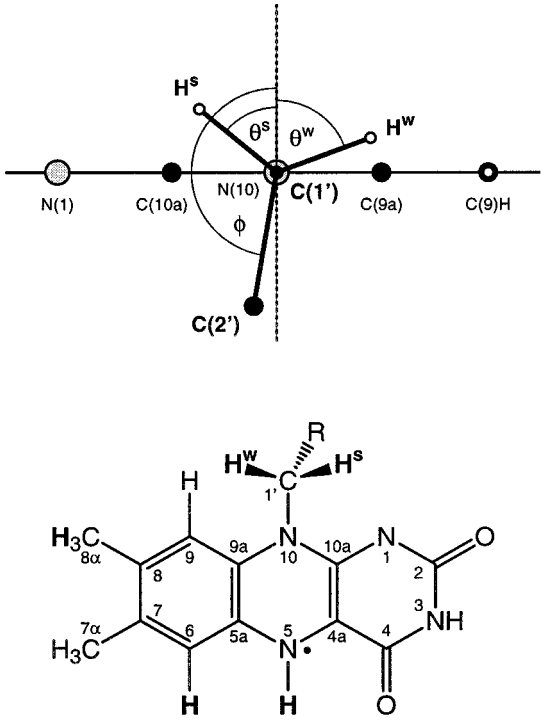

FIGURE 7: Structural model for the binding of the hydroxy alkyl side chain to the isoalloxazin moiety of FAD viewed along the C(1′)−N(10) bond. θ^w, θ^s and ϕ are the dihedral angles between the direction perpendicular to the molecular plane of the isoalloxazine moiety and the C(1′)−H^w, C(1′)−H^s, and C(1′)−C(2′) bonds, respectively.

$2p_z$-orbital of N(10). We have compared this angle with those obtained from the X-ray crystallography for both organisms: While the agreement with the DNA photolyase structure from *E. coli* is only satisfactory (166.2°), the *A. nidulans* structure provides an excellent fit (170.3°) to our findings. It is interesting to note, that in neutral flavin semiquinones in vitro dihedral angles close to $\phi = 180°$ are achieved. Apparently, the protein environment forces the isoalloxazin ring into a specific conformation with respect to the ribityl side chain. This might be important for the function of the enzyme.

CONCLUSIONS

In the present study, we have shown that high-resolution ENDOR and TRIPLE resonance in conjunction with EPR spectroscopy at different field and frequency ranges can be successfully applied to elucidate the electronic spin distribution of the flavin cofactor in DNA photolyase. The hfc's of the protons at C(8α) and C(6) represent sensitive probes for the spin density distribution on the benzene ring of the isoalloxazin moiety. They show that the unpaired electron is very much more localized in DNA photolyase than in other flavoenzymes. The ratio of the isotropic hfc's of the two inequivalent protons at C(1′) was used as a structural tool to characterize the linkage of the isoalloxazine ring system to the hydroxyalkyl side chain with high precision. It is expected that, when the DNA substrate binds to the photolyase enzyme, both the electronic and geometric structure of the FAD cofactor will be altered, reflecting specific changes in the protein environment. Studies along these lines together with model calculations based on the density functional theory formalism are currently in progress and will be published elsewhere.

ACKNOWLEDGMENT

We thank Professor Harry Kurreck (Free University Berlin, Germany) and Dr. Robert Bittl (Technical University Berlin, Germany) for valuable discussions. It is a pleasure to thank Jakob Lopez for his assistance during the initial experiments.

REFERENCES

1. Zhao, X., and Mu, D. (1998) *Histol. Histopathol. 13*, 1179−1182.
2. Heelis, P. F., Hartman, R. F., and Rose, S. D. (1996) *J. Photochem. Photobiol. A Chem. 95*, 89−98.
3. Heelis, P. F., Hartman, R. F., and Rose, S. D. (1995) *Chem. Soc. Rev. 24*, 289−297.
4. Sancar, A. (1994) *Biochemistry 33*, 2−9.
5. Sancar, A. (1996) *Science 272*, 48−49.
6. Sancar, A. (1992) in *Advances in Electron-Transfer Chemistry* (P. E. Mariano, ed.) Vol. 2, pp 215−272, JAI Press: London.
7. Todo, T. (1999) *Mutat. Res. 434*, 89−97.
8. Miyamoto, Y., and Sancar, A. (1998) *Proc. Natl. Acad. Sci. U.S.A. 95*, 6097−6102.
9. Zhao, S., and Sancar, A. (1997) *Photochem. Photobiol. 66*, 727−731.
10. Park, H.-W., Kim, S.-T., Sancar, A., and Deisenhofer, J. (1995) *Science 268*, 1866−1872.
11. Tamada, T., Kitadokoro, K., Higuchi, Y., Inaka, K., Yasui, A., de Ruiter, P. E., Eker, A. P. M., and Miki, K. (1997) *Nature Struct. Biol. 4*, 887−891.
12. Kim, S.-T., and Sancar, A. (1993) *Photochem. Photobiol. 57*, 895−904.
13. Gindt, Y. M., Vollenbroek, E., Westphal, K., Sackett, H., Sancar, A., and Babcock, G. T. (1999) *Biochemistry 38*, 3857−3866.
14. Aubert, C., Mathis, P., Eker, A. P. M., and Brettel, K. (1999) *Proc. Natl. Acad. Sci. U.S.A. 96*, 5423−5427.
15. Rustandi, R. R., and Jorns, M. S. (1995) *Biochemistry 34*, 2284−2288.
16. Essenmacher, C., Kim, S.-T., Atamian, M., Babcock, G. T., and Sancar, A. (1993) *J. Am. Chem. Soc. 115*, 1602−1603.
17. Kim, S.-T., Sancar, A., Essenmacher, C., and Babcock, G. T. (1993) *Proc. Natl. Acad. Sci. U.S.A. 90*, 8023−8027.
18. Kim, S.-T., Sancar, A., Essenmacher, C., and Babcock, G. T. (1992) *J. Am. Chem. Soc. 114*, 4442−4443.
19. Weil, J. A., Bolton, J. R., and Wertz, J. E. (1994) *Electron Paramagnetic Resonance*, John Wiley & Sons: New York.
20. Jorns, M. S., Sancar, G. B., and Sancar, A. (1984) *Biochemistry 23*, 2673−2679.
21. Piekara-Sady, L., and Kispert, L. D. (1994) in *Handbook of Electron Spin Resonance* (C. P. Poole, and H. A. Farach, Eds.), Chapter 5, pp 311−357, AIP Press: New York.
22. Möbius, K., Plato, M., and Lubitz, W. (1982) *Phys. Rep. 87*, 171−208.
23. Zamenhof, P. J., and Villarejo, M. (1972) *J. Bacteriol. 110*, 171−178.
24. Hennecke, H., Günther, I., and Binder, F. (1982) *Gene 19*, 231−234.
25. Stüber, D., Matile, H., and Garotta, G. (1990) *Immunol. Methods 4*, 121−152.
26. Richter, G., Fischer, M., Krieger, C., Eberhardt, S., Lüttgen, H., Gerstenschläger, I., and Bacher, A. (1997) *J. Bacteriol. 179*, 2022−2028.
27. Sancar, G. B., Smith, F. W., Lorence, M. C., Rupert, C. S., and Sancar, A. (1984) *J. Biol. Chem. 259*, 6033−6038.
28. Burghaus, O., Rohrer, M., Götzinger, T., Plato, M., and Möbius, K. (1992) *Meas. Sci. Technol. 3*, 765−774.
29. Prisner, T. F., Rohrer, M., and Möbius, K. (1994) *Appl. Magn. Reson. 7*, 167−183.

30. Ehrenberg, A., Müller, F., and Hemmerich, P. (1967) *Eur. J. Biochem. 2*, 286−293.
31. Müller, F., Hemmerich, P., Ehrenberg, A., Palmer, G., and Massey, V. (1970) *Eur. J. Biochem. 14*, 185−196.
32. Kurreck, H., Bock, M., Bretz, N., Elsner, M., Kraus, H., Lubitz, W., Müller, F., Geissler, J., and Kroneck, P. M. H. (1984) *J. Am. Chem. Soc. 106*, 737−746.
33. McConnell, H. M., Heller, C., Cole, T., and Fessenden, R. W. (1960) *J. Am. Chem. Soc. 82*, 766−775.
34. Bretz, N. H., Henzel, N., Kurreck, H., and Müller, F. (1989) *Isr. J. Chem. 29*, 49−55.
35. Çinkaya, I., Buckel, W., Medina, M., Gómez-Moreno, C., and Cammack, R. (1997) *Biol. Chem. 378*, 843−849.
36. Medina, M., Vrielink, A., and Cammack, R. (1994) *Eur. J. Biochem. 222*, 941−947.
37. Medina, M., Gómez-Moreno, C., and Cammack, R. (1995) *Eur. J. Biochem. 227*, 529−536.
38. Kurreck, H., Bretz, N. H., Helle, N., Henzel, N., and Weilbacher, E. (1988) *J. Chem. Soc., Faraday Trans. 1 84*, 3293−3306.
39. Heller, C., and McConnell, H. M. (1960) *J. Chem. Phys. 32*, 1535−1539.
40. Horsfield, A., Morton, J. R., and Whiffen, D. H. (1961) *Mol. Phys. 4*, 425−431.

BI991442U